BMC Genomics

RESEARCH Open Access

Identifying potential anthocyanin biosynthesis regulator in Chinese cherry by comprehensive genome-wide characterization of the *R2R3-MYB* transcription factor gene family

Yan Wang[1,2†], Hongxia Tu[1†], Jing Zhang[1], Hao Wang[1], Zhenshan Liu[1], Jingting Zhou[1], Wen He[1,2], Yuanxiu Lin[1], Yunting Zhang[1], Mengyao Li[1], Zhiwei Wu[1], Qing Chen[1,2], Yong Zhang[1], Ya Luo[1], Haoru Tang[1] and Xiaorong Wang[1,2*]

Abstract

Background Chinese cherry [*Cerasus pseudocerasus* (Lindl.) G.Don] (syn. *Prunus pseudocerasus* Lindl.) is an economically important fruiting cherry species with a diverse range of attractive colors, spanning from the lightest yellow to the darkest black purple. However, the MYB transcription factors involved in anthocyanin biosynthesis underlying fruit color variation in Chinese cherry remain unknown.

Results In this study, we characterized the *R2R3-MYB* gene family of Chinese cherry by genome-wide identification and compared it with those of 10 Rosaceae relatives and *Arabidopsis thaliana*. A total of 1490 R2R3-MYBs were classified into 43 subfamilies, which included 29 subfamilies containing both Rosaceae *MYBs* and *AtMYBs*. One subfamily (S45) contained only Rosaceae *MYBs*, while three subfamilies (S12, S75, and S77) contained only *AtMYBs*. The variation in gene numbers within identical subfamilies among different species and the absence of certain subfamilies in some species indicated the species-specific expansion within *MYB* gene family in Chinese cherry and its relatives. Segmental and tandem duplication events primarily contributed to the expansion of Chinese cherry *R2R3-CpMYBs*. The duplicated gene pairs underwent purifying selection during evolution after duplication events. Phylogenetic relationships and transcript profiling revealed that *CpMYB10* and *CpMYB4* are involved in the regulation of anthocyanin biosynthesis in Chinese cherry fruits. Expression patterns, transient overexpression and VIGS results confirmed that *CpMYB10* promotes anthocyanin accumulation in the fruit skin, while *CpMYB4* acts as a repressor, inhibiting anthocyanin biosynthesis of Chinese cherry.

Conclusions This study provides a comprehensive and systematic analysis of *R2R3-MYB* gene family in Chinese cherry and Rosaceae relatives, and identifies two regulators, *CpMYB10* and *CpMYB4*, involved in anthocyanin

†Yan Wang and Hongxia Tu contributed equally to this work.

*Correspondence:
Xiaorong Wang
wangxr@sicau.edu.cn

Full list of author information is available at the end of the article

biosynthesis in Chinese cherry. These results help to develop and utilize the potential functions of anthocyanins in Chinese cherry.

Keywords Chinese cherry, Fruit color, Genome-wide identification, R2R3-MYB transcription factor, Regulation of anthocyanin biosynthesis, *CpMYB10*, *CpMYB4*

Introduction

Chinese cherry [*Cerasus pseudocerasus* (Lindl.) G.Don] (syn. *Prunus pseudocerasus* Lindl.), belonging to the Rosaceae family, is an economically important tetraploid fruiting cherry species [1–3]. Cherry cultivation has been rapidly developing in China and has increasingly contributed to poverty alleviation and rural revitalization. Chinese cherry exhibits a wide range of fruit colors, including yellow, vermilion on yellow ground, red, purple red, and black purple [4]. The fruit coloration is attributed to the accumulation of anthocyanins, which are controlled by a distinct group of R2R3-MYB transcription factors [5, 6]. In apple, *MdMYB10*, *MdMYB1*, and *MdMYBA* are the main determinants of fruit color variations among cultivars [7–9]. In sweet cherry, three *PavMYB10.1* alleles determine the fruit skin color: yellow (*PavMYB10.1c*), blush (homozygous for *PavMYB10.1b*) and red (at least one intact *PavMYB10.1a*) [10]. Allelic variation of *MYB10* is the major force controlling natural variations in both skin and flesh color in strawberry fruits [11]. Therefore, R2R3-MYB TFs play key roles in regulating the anthocyanin biosynthesis in Rosaceae fruit crops.

Numerous reports have demonstrated that the R2R3-MYB TFs typically form a well-conserved MYB-bHLH-WD40 (MBW) complex to regulate the anthocyanin biosynthesis [12–14]. In *Arabidopsis*, *AtMYB11/12/111* independently participate in transcriptional activation of the early biosynthetic genes (EBGs), while *AtMYB75/90/113/114* of subfamily S6 activate the late biosynthetic genes (LBGs) by the formation of MBW complex [15]. These functions are conserved in other species, such as apple *MdMYB10* [16, 17], strawberry *FvMYB10* [11, 18] and *FaMYB5* [19], and sweet cherry *PavMYB10* and *PacMYBA* [10, 20, 21]. In addition to MYB activators, it has been reported that R2R3-MYB TFs belonging to subfamily S4 can repress anthocyanin accumulation. Two types of MYB repressors have been identified, one of which is dependent on its own EAR (ERF-associated amphiphilic repression) inhibitory sequence, while the other is independent [22–24]. Furthermore, two ways to inhibit anthocyanin biosynthesis have been proposed: the AtMYB4-like type [25] and the FaMYB1-like type [26]. The AtMYB4-like type acts directly on the promoters of target structural genes [27], such as *MdMYB6*, *MdMYB16* in apple [24, 28] and *SlMYB7* in tomato [29]. The FaMYB1-like type functions as a corepressor, which is incorporated into or binds MBW complexes to alter the complex activity and transform from activation to inhibition [27], including grape *VvMYBC2*, *VvMYBC2-L3*, and apple *MdMYB15L* [23, 30, 31]. These findings have highlighted the core roles of transcriptional regulations of R2R3-MYB in the control of anthocyanin biosynthesis.

In Chinese cherry, cyanidin and its glycoside derivatives have been identified as the primary anthocyanins responsible for fruit coloration [32–34]. Compared to yellow fruits, (dark)-red fruits were found to accumulate significantly higher level of cyanidin-3-rutinoside, but lower levels of flavanol and proanthocyanidin [33]. The up-regulation of structural genes in cyanidin biosynthesis, including EBGs (*CpF3H*, *CpF3'H*) and LBGs (*CpDFR*, *CpANS*, and *CpUFGT*), was observed, contributing to the formation of dark-red fruits [33]. On the contrary, higher expression of *CpLAR* was observed in yellow fruits. In addition, eight regulatory genes, including MYB TFs, have been identified as candidate determinants of fruit color in Chinese cherry [33]. However, the genome-wide characterization of *MYB* gene family and their regulatory roles in anthocyanin biosynthesis in Chinese cherry has not been previously reported.

To gain further insights into the regulatory network underlying fruit color variation in Chinese cherry, we conducted a genome-wide characterization of the R2R3-MYB gene family in Chinese cherry and relative species in Rosaceae family. Based on transcriptomic profiling and function verification, we identified the key genes involved in anthocyanin biosynthesis in Chinese cherry fruits. Our objectives were (i) to characterize the *R2R3-MYB* gene family of Chinese cherry through genome-wide identification and compare it with that of 10 Rosaceae relatives and *Arabidopsis thaliana*; (ii) to identify key MYB TFs related to anthocyanin biosynthesis in Chinese cherry; and (iii) to preliminarily verify the functions of *CpMYB10* and *CpMYB4*. This study provides a starting point for further analysis of MYB functions in Chinese cherry and establishes a solid foundation for utilizing candidate genes in breeding programs aimed at improving anthocyanin accumulation.

Materials and methods

Plant materials

Three Chinese cherry accessions, namely 'PZB', 'HF' and 'HP600', representing yellow, red and black-purple fruit colors respectively, were used in this study. They were cultivated under field conditions at Cherry Germplasm Repository of Sichuan Province in Sichuan Agricultural

University (Chengdu), China. The fruits from three accessions were harvested at full maturity stage. Tissue samples including roots, stems, leaves, flower buds (red), and open flowers (white) were specifically collected from 'HF' accession. All samples were immediately frozen in liquid nitrogen and stored at −80 °C for subsequent analysis, with three biological replicates per sample.

Determination of fruit color and total anthocyanin content

Fruit color parameters (lightness L*, redness a*, and yellowness b*) were measured using a KONICA MINOLTA CM-2600d spectrophotometer (Japan), and the color ratio (a*/b*) was calculated [35]. Ten cherries for each replicate were used, with three biological replicates per sample point.

Total anthocyanin content was determined using the pH differential method described by Lee et al. [36]. Approximately 0.5 g of fruit tissue was extracted with 5 mL of extraction solution (acetone: methanol: water: acetic acid=2:2:1:0.5) and heated in a water bath at 40 °C. The mixture was centrifuged at 8,000 ×g for 25 min, and the supernatant was used for analysis. Two buffer systems were used with 0.4 M potassium chloride (pH 1.0) and 0.4 M dibasic sodium (pH 4.5). The total anthocyanin content was calculated using the equation: $A = [(A_{510}-A_{700})\ pH_{1.0} - (A_{510}-A_{700})\ pH_{4.5}]$ and converted into mg cyanidin 3-glucoside per 1,000 g fresh weight ($mg{\cdot}kg^{-1}$ FW). Three independent biological replicates per sample point were analyzed.

Genome-wide identification of R2R3-MYB gene family

A total of 12 genomes from Chinese cherry (unpublished) and related species within Rosaceae family, and *Arabidopsis thaliana* were selected for analysis (Table 1).

Putative MYB proteins were identified using a Hidden Markov Model (HMM) profile of the MYB DNA binding domain (PF00249) (http://pfam.sanger.ac.uk/) and conserved domains were confirmed using SMART (http://smart.embl-heidelberg.de/) and Pfam (http://pfam.janelia.org/). The ExPASy proteomics tool (http://web.expasy.org) was utilized to predict the protein characteristics, including the number of amino acids, molecular weight, theoretical isoelectric point (pI), instability index (II), aliphatic index (AI), and grand average of hydropathicity (GRAVY). Then a neighbor-joining (NJ) phylogenetic tree was constructed by aligning the full-length MYB amino acid sequences using MAFFT and MEGAX 11, with 1,000 replicate bootstraps. The resulting tree was visualized using the Chiplot online tool (https://www.chiplot.online/). The classification and biological functions of the R2R3-MYBs were determined based on their phylogenetic relationships with the corresponding AtMYB proteins.

The chromosomal distribution of *CpMYB* gene family in the Chinese cherry genome was depicted using TBtools [48]. Gene duplication events were analyzed using the MCScanX (http://chibba.pgml.uga.edu/mcscan2). Gene pair collinearity analysis of *CpMYBs* was illustrated using the Circos software (http://circos.ca/software/download/). Non-synonymous (Ka) and synonymous (Ks) substitutions of gene pairs were calculated

Table 1 The information of reference genomes for Chinese cherry and other eleven species

Species	Release	Source	References
Cerasus pseudocerasus	'Luoyang Guying'	In the lab	Unpublished
Relatives			
Subfamily Amygdaloideae			
Tribe Amygdaleae			
Cerasus avium	*Prunus avium* cv. Tieton Genome v2.0 Assembly & Annotation	GDR database	[37]
Cerasus yedoensis	*Prunus yedoensis* var. *nudiflora* Genome v1.0 Assembly & Annotation	GDR database	[38]
Cerasus serrulata	-	GDR database	[39]
Prunus salicina	*Prunus salicina* Sanyueli FAAS Whole Genome v1.0 Assembly & Annotation	GDR database	[40]
Armeniaca vulgaris	*Prunus armeniaca* cv. Stella Whole Genome v1.0 Assembly & Annotation	GDR database	[41]
Amygdalus persica	*Prunus persica* Whole Genome Assembly v2.0 & Annotation v2.1 (v2.0.a1)	GDR database	[42]
Tribe Maleae			
Pyrus pyrifolia	*Pyrus pyrifolia* Whole Genome v1.0 Assembly & Annotation	GDR database	[43]
Malus domestica	*Malus domestica* cv. Gala	http://bioinfo.bti.cornell.edu/apple_genome	[44]
Subfamily Rosoideae			
Tribe Potentilleae			
Fragaria vesca	*Fragaria vesca* Whole Genome v4.0.a1 Assembly & Annotation	GDR database	[45]
Tribe Rubeae			
Rubus occidentalis	*Rubus occidentalis* Whole Genome v3.0 Assembly & Annotation	GDR database	[46]
Arabidopsis thaliana	https://www.arabidopsis.org/	TAIR database	[47]

with TBtools [48, 49]. Conserved domains and motifs were predicted using MEME Suite v5.4.1 (https://meme-suite.org/meme/tools/meme), and an intron-exon structure diagram in Chinese cherry was generated using TBtools. The subcellular localization was predicted using the Plant-mPLoc website (http://www.csbio.sjtu.edu.cn/bioinf/plant-multi/). *Cis*-elements in the promoter region in the 2000 bp upstream sequences were obtained from the PlantCARE database (http://bioinformatics.psb.ugent.be/webtools/plantcare/html/).

Transcriptome analysis and RT-qPCR validation

A detailed understanding of *CpMYB* gene expression underlying fruit development (S1-S5) in yellow and red fruits [33] is necessary. The transcriptomic data were retrieved from the CNGB database (https://db.cngb.org/cnsa/experiment/page/batch/sub037808/view/) under accession number CNP0003682. A heat map of gene expression was generated using TBtools software. Weighted gene co-expression network analysis (WGCNA) was further performed using the WGCNA R package (v1.4.17) to identify core gene modules and hub genes related to anthocyanin biosynthesis. All differentially expressed genes were imported into the R package and used to construct gene co-expression modules via an automatic module building function. An adjacency matrix was then created to illustrate the correlation strength between the modules and color-related characteristics, including a^*, b^*, L^*, a^*/b^* ratio, and anthocyanin content. Genes associated with trait-related modules were extracted for further analysis.

RT-qPCR-based expression analysis was carried out using TransStart®Green qPCR SuperMix (TransGen Biotech Co., Ltd, Beijing, China) on a CFX96 Touch™ Real-Time PCR system (Bio-Rad, Hercules, CA, USA). Total RNA was extracted using the AFTSpin Uninersal Plant Fast RNA Extraction Kit (ABclonal, Wuhan, China). The cDNA was synthesized from RNA using the PrimeScript™ RT-PCR Kit (RR047A; TaKaRa Bio, Kusatsu, Japan). The primers were designed using Primer Premier 5 software (Table S1). The RT-qPCR reaction procedure was as follows: 95℃ for 30 s, followed by 40 cycles of 95℃ for 5 s, 60℃ for 30 s, and 72℃ for 30 s. The relative expression was calculated using the $2^{-\Delta\Delta Ct}$ method, with *β-Actin* as the internal reference.

Subcellular localization

The empty vector was linearized through double enzyme digestion using XbaI and BamHI enzymes for the subcellular localization vector. The CDS of *CpMYB10/4* were amplified and inserted into pYTSL-16 (modified from pMDC83-35 S and pSITE-2NB) using the CloneExpress II One Step Cloning Kit (Vazyme, Nanjing, China). We created a plasmid that encoded a fusion protein of CpMYB10/4 and green fluorescent protein (GFP), driven by the 35 S promoter. Subsequently, the plasmid was transformed into *Agrobacterium tumefaciens* strain GV2301. The empty-GFP vector was used as a negative control. The constructs were transiently expressed in tobacco leaves for subcellular localization analysis. The primers for the eGFP fusion vector are listed in Table S1.

Transcriptional activation assay

The full-length sequence of *CpMYB10/4* was cloned and inserted into pGBKT7, with the specific primer sequences listed in Table S1. The positive control (pGBKT7-p53), negative control (pGBKT7-lam), and recombinant vector (pGBKT7-CpMYB10/4) were transformed into *Saccharomyces cerevisiae* strain Y2H-Gold. The transformed cells were incubated on SD-/Trp and SD-/Trp/Ade/His media supplemented with 40 μg/μL X-α-Gal at 30 °C for 3 ~ 7 days. Transactivation activity was assessed by observing the growth of the transformed cells.

Transient overexpression and virus-induced gene silencing

The full length of CDS sequences of both *CpMYB10* and *CpMYB4* were cloned into pCAMBIA2301 and pTRV2 vectors using Takara PrimerSTAR Max DNA Polymerase (Takara, Beijing, China) and specific primers (Table S1). The pCAMBIA2301 fusions *CpMYB10* and *CpMYB4* were introduced into yellow fruits via *Agrobacterium*-mediated genetic transformation [50]. The recombinant plasmids pTRV-*CpMYB10* and -*CpMYB4* were transformed into *Agrobacterium tumefaciens* strain GV2301 through electroporation. TRV-mediated gene-silencing of *CpMYB4* and *CpMYBB10* was performed as previously described with slight modifications [51] for yellow and red fruits, respectively. The fruits selected for infiltration were at the pre-color conversion stage (approximately DAF33 ~ 36). The fruits were infiltrated using needleless syringes into their skin surface. After seven days of infiltration, fruits were harvested to measure color-related characteristics. Both overexpression and silencing assays were performed, involving 40 transformed fruit per strain from the same tree every time, with three biological replicates using three 8-year-old trees (Table S2).

Data analysis

The experimental data were recorded as mean values ± standard deviation (SD). The statistical differences were analyzed using Prism 9 software. The differences between groups were determined using Student's t-test. The results with a p value below 0.05 were considered statistically significant.

Results

Comprehensive genome-wide identification of *R2R3-MYB* gene family

R2R3-MYB gene family in Chinese cherry, 10 Rosaceae relatives and Arabidopsis thaliana

A total of 191 *CpMYB* genes were identified in Chinese cherry, with the R2R3 type (99 genes) comprising the largest proportion at 51.83% of the total number (Table S3). Additionally, 85 *1R-CpMYB* genes, 4 *3R-CpMYB* genes, and 3 *4R-CpMYB* genes were also obtained. Similar strategies were used to identify *R2R3-MYB* genes among 10 Rosaceae relatives: 108 in *C. avium*, 134 in *C. yedoensis*, 111 in *C. serrulata*, 118 in *P. salicina*, 113 in *A. vulgaris*, 110 in *A. persica*, 193 in *P. pyrifolia*, 177 in *M. domestica*, 103 in *F. vesca*, and 98 in *R. occidentalis* (Table S4). The results revealed that the number of *R2R3-MYB* genes was much greater in tribe Maleae than those in the other three tribes, and *Arabidopsis*.

These R2R3-MYB proteins were classified into 43 subfamilies (Fig. 1A) based on the NL tree topology and subfamily classification in *Arabidopsis*. They included 42 major subfamilies found in *Arabidopsis* and an additional subfamily (S45) belonging to Rosaceae family [6, 52]. Different subfamilies contained varying numbers of genes, ranging from 12 for S10 to 97 for S14 (with only 6, 1, and 1 for S12, S75, and S77 respectively). The sizes of these subfamilies also varied greatly within and between tribes (Fig. 1B). For instance, tribe Maleae exhibited a higher number of members compared to other tribes, particularly in subfamilies S21, S15, S20, S8, S31, S36, and S1, while a similar number of members was observed for subfamilies S6, S44, S7, and S4. The number in the majority of subfamilies such as S21, S6, S4, S30, and S74 in Chinese cherry was less than that in the other three *Cerasus* species. It is worth noting that subfamilies S19, S13, and S10 exist in all species except for Chinese cherry, suggesting that these *CpMYB* genes may have evolved or been lost during the divergence process. A similar phenomenon is also observed in other species, such as S28 being absent in *A. vulgaris* and *A. persica*, S15 and S31 absent in *C. serrulata* and *R. occidentalis*, as well as S74 absent in *F. vesca*. In addition, subfamily S45 is represented in all Rosaceae species but not in *Arabidopsis*. The subfamilies S12, S75, and S77 are all absent in Chinese cherry and any other Rosaceae species. These results possibly imply species-specific differences for some MYB subfamilies in Chinese cherry and its Rosaceae relatives.

Overall, the functions of *R2R3-MYB* gene family in Chinese cherry and its relatives can be categorized into three major processes: development and cell differentiation, specialized metabolism (particularly the phenylpropanoid biosynthesis pathway), and stress responses (biotic and abiotic stresses) (Fig. 1B). Previous studies suggested that the *R2R3-MYB* genes within the same subfamily may have similar functions [53]. For example, the subfamilies S45 and S5 genes are involved in proanthocyanidin biosynthesis, while S7 members are involved in flavonoid biosynthetic pathway. Equivalent or similar biological functions can be controlled by different subfamilies of MYB TFs. Members from eight subfamilies (S21, S3, S8, S13, S32, S30, S31, and S10) regulate secondary cell wall biosynthesis. Additionally, genes in subfamilies S6 and S4 participate in the regulation of anthocyanin biosynthesis (Fig. 1B).

Characterization of R2R3-MYBs in Chinese cherry

A total of 99 *R2R3-CpMYB* genes were identified in Chinese cherry, and their detailed information was summarized in Table S5. These CpMYB proteins exhibited significant variation in characteristics, with protein length ranging from 106 to 1206 amino acids, molecular weight ranging from 12.83 to 134.89 kDa, and theoretical isoelectric point ranging from 4.83 to 10.74. These proteins were predicted to localize in the nuclear region (Table S5). Through chromosomal localization analysis, the *CpMYB* genes were unevenly distributed across all eight chromosomes (Fig. 2A). Chromosome 1 had the greatest number of *CpMYB* genes (20 in total), followed by chr3 (19 genes) and chr6 (16 genes). The least number of *CpMYB* genes was on chr8, with only four genes. Co-linearity analysis revealed the identification of 31 duplication pairs, consisting of 26 segmental duplication pairs and five tandem duplication pairs (Fig. 2B). The Ks value ranged from 0.0004 to 4.3882 (Table S6), showing a wider range than sweet cherry MYB family [54]. Eight duplicated genes showed relatively high Ks values (1.8032 ~ 4.3882), indicating that more ancient duplication events occurred in Chinese cherry than in sweet cherry (Ks: 0.5875 ~ 1.6836, 32.28 ~ 92.50 Mya) [54] and apple (Ks: 1.5 ~ 1.8, ~ 140 Mya) [55]. The Ka/Ks ratios of 26 duplication gene pairs were all less than 0.8, indicating that these *R2R3-CpMYB* genes have experienced purifying selection during evolution following duplication events.

The amino acid sequences of the R2 and R3 MYB repeats were extracted from R2R3-CpMYB proteins (Fig. S1). In the R2 domain, three Trp residues were spaced by 19 amino acids. In the R3 domain, the Trp residues were separated by 18 amino acids, with the first being replaced by some hydrophobic amino acids. A total of 20 diverse motifs were identified in CpMYB proteins, with each motif ranging in size from 8 to 50 (Table S7). Generally, genes within the identical subfamily exhibited conserved motif patterns (Fig. S2A-B). Across all members, the motifs at the N-terminus were relatively conserved, including motifs 1 ~ 5, and motif 7, which encode the conserved MYB DNA-binding domain. Most subfamilies had exclusive motifs, but some motifs overlapped

A

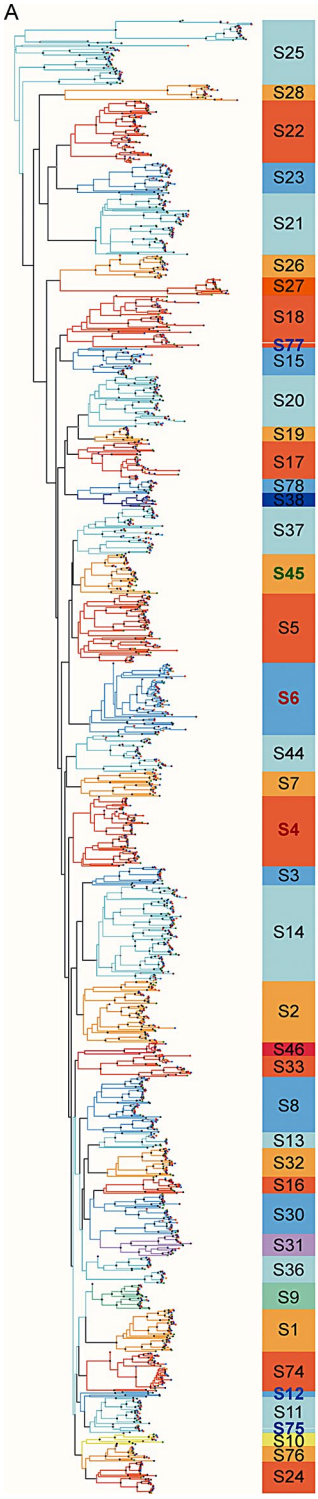

B

Subfamily	Function	Number												Total
		Cp	Ca	Cy	Cs	Ps	Av	Ap	Pp	Md	Fv	Ro	At	
S25	Embryogenesis; glucosinolate pathway	**5**	2	7	6	4	4	4	8	8	5	5	7	65
S28	Stomatal formation; female reproductive development	**1**	1	3	1	1	**0**	**0**	3	2	1	1	2	16
S22	Abiotic stress	**6**	5	4	5	5	5	5	9	5	5	5	4	63
S23	Abiotic stress	**3**	2	3	2	2	2	2	4	4	2	2	3	31
S21	Secondary cell wall biosynthesis	**3**	5	7	4	4	4	3	8	8	4	4	8	62
S26	Sperm-cell formation; pollen formation	**2**	1	2	1	3	2	2	3	3	2	2	1	24
S27	Leaf patterning; stem cell function	**2**	**0**	1	1	1	1	1	3	1	3	2	1	17
S18	Anther/pollen development	**3**	5	3	3	5	4	4	6	7	4	2	7	52
S77	**Pollen mitosis I and cell lineage formation**	**0**	**0**	**0**	**0**	**0**	**0**	**0**	**0**	**0**	**0**	**0**	**1**	**1**
S15	Vegetative development	**1**	2	4	**0**	2	2	2	5	6	1	**0**	3	28
S20	Abiotic stress	**2**	4	3	3	4	4	4	7	7	4	4	6	52
S19	Stamen development; anther development	**0**	1	1	1	1	1	1	2	2	1	1	3	15
S17	Abiotic stress	**3**	2	3	3	5	3	3	4	6	2	1	3	38
S78	Abiotic stress	**1**	2	1	**0**	**0**	1	1	2	2	1	1	2	14
S38	Polyphenol biosynthesis	**1**	1	3	1	1	1	1	1	1	1	1	1	14
S37	Trichome development	**5**	4	7	3	4	4	4	6	6	2	2	1	48
S45	**Proanthocyanidin pathway**	**3**	**3**	**3**	**3**	**2**	**3**	**3**	**5**	**5**	**7**	**3**	**0**	**40**
S5	Proanthocyanidin biosynthesis	**5**	6	5	5	5	6	6	9	8	9	5	1	70
S6	**Anthocyanin biosynthesis**	**5**	**7**	**6**	**8**	**8**	**7**	**7**	**8**	**7**	**2**	**4**	**4**	**73**
S44	Proanthocyanindins and mucilage biosynthesis; anthocyanin; biotic stress	**3**	3	2	4	3	3	3	5	3	4	3	1	37
S7	Flavonoid biosynthesis	**2**	2	1	2	2	2	2	2	4	2	1	3	25
S4	**Inhibit anthocyanin biosynthesis and flower development**	**4**	**7**	**7**	**5**	**6**	**6**	**6**	**8**	**9**	**3**	**4**	**6**	**71**
S3	Flavonoid and lignin biosynthesis	**3**	1	1	1	1	1	1	2	2	1	1	4	19
S14	Vegetative development	**7**	6	11	10	7	7	7	13	10	6	7	6	97
S2	Abiotic stress	**5**	4	5	4	6	5	5	9	6	5	5	3	62
S46	Pollen and anther development	**1**	**0**	1	**0**	1	1	1	2	2	**0**	2	1	12
S33	Anther development	**1**	1	2	2	2	2	2	4	2	2	2	1	23
S8	Secondary cell wall biosynthesis	**3**	4	4	5	4	4	4	8	7	3	4	6	56
S13	Lignin biosynthesis; stomatal closure	**0**	1	1	1	1	1	1	2	2	1	1	4	16
S32	Secondary cell wall biosynthesis	**2**	3	2	1	3	2	2	4	4	2	2	2	29
S16	Response to far-red light	**1**	1	1	1	1	1	1	2	2	1	2	3	17
S30	Cell wall thickening in fiber cells and secondary wall deposition in anthers	**2**	4	3	4	3	3	3	5	4	3	5	2	41
S31	Secondary cell wall biosynthesis	**1**	1	2	**0**	2	3	2	4	4	2	**0**	1	22
S36	Inflorescence development; seed germination	**1**	2	3	3	2	2	2	4	4	2	2	1	28
S9	Epidermal cell outgrowth	**2**	2	1	2	2	2	2	4	3	2	2	2	26
S1	Abiotic stress	**2**	2	4	3	3	3	3	6	6	3	3	5	43
S74	Unknown	**3**	4	6	6	5	4	3	3	3	**0**	1	2	40
S12	**Glucosinolate biosynthesis**	**0**	**0**	**0**	**0**	**0**	**0**	**0**	**0**	**0**	**0**	**0**	**6**	**6**
S11	Abiotic stress	**2**	3	3	2	3	3	3	5	5	2	1	3	35
S75	**Regulate cadmium accumulation**	**0**	**0**	**0**	**0**	**0**	**0**	**0**	**0**	**0**	**0**	**0**	**1**	**1**
S10	Suberin biosynthesis and deposition	**0**	1	1	1	1	1	1	1	1	1	1	2	12
S76	Regulate suberization in Arabidopsis roots	**1**	1	4	1	1	1	1	2	2	1	1	1	17
S24	Root development	**2**	2	3	3	2	2	2	5	4	1	3	3	32
Total		**99**	108	134	111	118	113	110	193	177	103	98	126	**1490**

Fig. 1 R2R3-MYB gene family in Chinese cherry and comparative analysis. (**A**) Classification of R2R3-MYB subfamilies based on phylogenetic relationships. (**B**) Functional annotation and gene number of R2R3-MYB subfamilies. Cp, *Cerasus pseudocerasus*; Ca, *C. avium*; Cy, *C. yedoensis*; Cs, *C. serrulata*; Ps, *Prunus salicina*; Av, *Armeniaca vulgaris*; Ap, *Amygdalus persica*; Pp, *Pyrus pyrifolia*; Md, *Malus domestica*; Fv, *Fragaria vesca*; Ro, *Rubus occidentalis*; At, *Arabidopsis thaliana*. The 126 R2R3 *AtMYBs* (excluding the CDC5 like proteins: S29) are clustered into 42 major subfamilies (S1-S28, S30-S33, S36-S38, S44, S46, and S74-S78) [6, 52]. Subfamily S45 is present in Rosaceae but absent in *Arabidopsis* [6], while S12, S75, and S77 are absent in Rosaceae. The subfamilies S6 and S4, highlighted in red font, are associated with anthocyanin biosynthesis

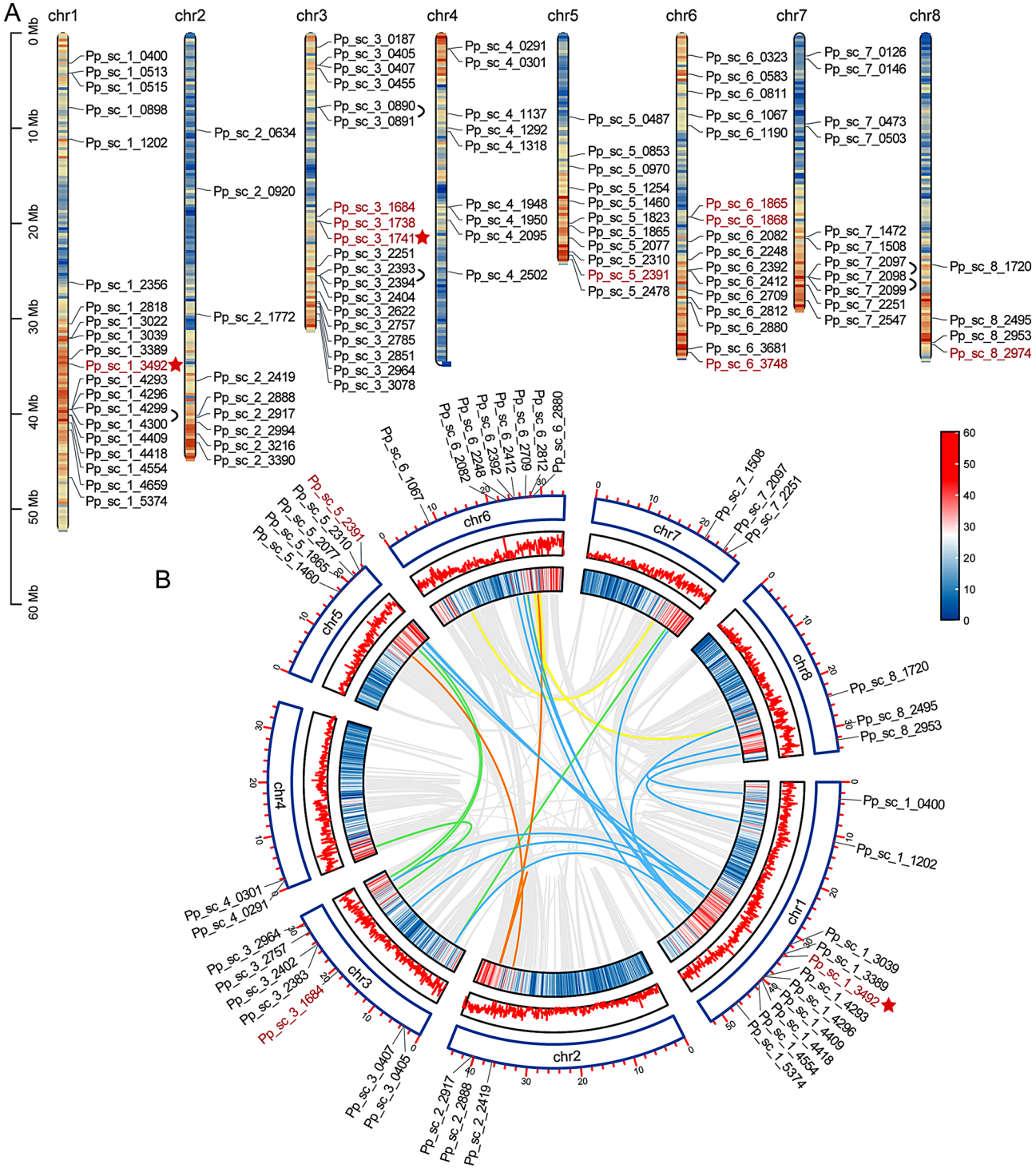

Fig. 2 Characterization of *R2R3-CpMYB* genes in Chinese cherry. (**A**) Chromosomal localization of *CpMYBs*. Red font represents the genes related to anthocyanin metabolism. Genes connected by right parentheses represent the tandem duplication pairs. (**B**) Segmental duplication and synteny analysis of *CpMYBs*. Duplicated gene pairs placed on the different chromosomes linked with colorful lines. Pp_sc: Ppseudocerasus_HiC_scaffold. The same as below

across subfamilies. For example, motif 16, 13 and 20 was exclusive to subfamily S6, S22 and S27 respectively, while motif 8 was found in most members among 12 subfamilies. The differences in the quantities and types of conserved motifs may result in changes in the degree of rate of evolution. Most genes within the same subfamily displayed common exon/intron organizations (Fig. S2C). The exon numbers ranged from 1 to 15 in Chinese

cherry, with 61.62% of genes containing three exons. Genes in subfamily S6 contained 2 introns and 3 exons, while members of subfamily S4 included 1 ~ 2 introns and 2 ~ 4 exons. Additionally, 6 members in subfamily S22 were intronless, and 52 CpMYB proteins had no untranslated region (UTR). The presence of identical motifs and exon/intron structures among genes suggested that they may have similar functions.

Various *cis*-regulatory elements were predicted in the promoter sequences, and a total of 56 types of *cis*-elements were identified (Table S8). These elements were divided into four groups: light responsive (29), plant growth (9), phytohormone responsive (13), and stress responsive (5) (Fig. S3). Light responsive *cis*-acting elements were found to be prevalent in the promoter regions, with the Box 4 (24.8%) and G-box (23.7%) being the most common. The O_2-site encompassed the highest proportion (34.3%), follow by CAT-box (24.5%), which are responsible for plant growth. The phytohormone response related *cis*-elements like ABRE (27.8%), ARE (21.0%), CGTCA (13.3%), and TGACG (13.3%) were also observed, which are linked with ABA, anaerobic induction, and MeJA responses. Furthermore, certain elements were found to be widely distributed in the promoter regions of most *CpMYBs*, with Box 4 being the most frequently distributed, followed by G-box and ABRE. These findings suggested that members of *CpMYB* gene family can be induced by light and ABA signals.

Key genes associated with anthocyanin biosynthesis in Chinese cherry fruits by transcriptome profiling

Expression patterns of R2R3-CpMYB genes

An expression heat map of *R2R3-CpMYB* genes was generated based on the FPKM values at different developmental stages of yellow ('PZB') and red ('HF') fruits (Fig. 3A, Table S9). They exhibited significantly different expression levels across these developmental stages. In most cases, genes with the same subfamily displayed similar expression patterns. For example, genes in subfamilies S23, S21, S37, S45, S32, S36, and S9 were predominantly expressed at green fruit stage. On the other hand, genes in subfamilies S6 and S3 showed relatively high expression level at fruit coloration stage. Duplicated genes with high sequence similarity, such as Ppseudocerasus_HiC_scaffold_1_4299 and 1_4300, exhibited different expression profiles. Notably, in subfamily S6, which promotes anthocyanin biosynthesis, the expression of Ppseudocerasus_HiC_scaffold_3_1741 increased with fruit development and was higher in red than in yellow fruits. In subfamily S4, which inhibits anthocyanin biosynthesis, Ppseudocerasus_HiC_scaffold_1_3492 was strongly expressed in matured yellow fruits. Its expression gradually increased with fruit development in yellow fruits, suggesting that the repressor was active during anthocyanin biosynthesis, providing feedback regulation.

Validation of candidate R2R3-CpMYB genes

To further confirm the genes involved in anthocyanin accumulation in Chinese cherry fruits, we conducted WGCNA based on the normalized expression data for 46,058 genes from all 30 samples. After filtering, 11,515 genes were retained and classified into 22 distinct gene modules (Fig. 3B, Fig. S4). The lightgreen module, consisting of 103 genes, and the greenyellow module, consisting of 226 genes, showed a significant positive correlation with a^* (r^2 = 0.68, 0.90), anthocyanin content (r^2 = 0.96, 0.84), and a^*/b^* ratio (r^2 = 0.97, 0.80). The KEGG pathway enrichment analysis revealed that the genes within the lightgreen module were significantly enriched in "flavonoid biosynthetic process", "regulation of anthocyanin biosynthetic process", and "anthocyanin-containing compound biosynthetic process". Furthermore, Ppseudocerasus_HiC_scaffold_3_1741 was specifically enriched in the "regulation of anthocyanin biosynthetic process" pathway (Fig. 3C). These findings suggested that Ppseudocerasus_HiC_scaffold_3_1741 may be involved in the biosynthesis of anthocyanins.

Ppseudocerasus_HiC_scaffold_3_1741/6_1865 (S6) and Ppseudocerasus_HiC_scaffold_1_3492/3_1684/8_2974 (S4), with normalized FPKM values greater than 1, were selected for RT-qPCR analysis (Fig. 3D). The results showed that the expression levels of Ppseudocerasus_HiC_scaffold_3_1741 in (dark)-red fruits were significantly higher by 5 ~ 6-fold than that in yellow fruits, consistent with the anthocyanin content in fruits (Fig. 3E). The expression of Ppseudocerasus_HiC_scaffold_3_1741 was higher in red flower buds than that in white blooming flowers, and other three tissues, suggesting that Ppseudocerasus_HiC_scaffold_3_1741 may also regulate the coloration of flower buds. In contrast, the expression level of Ppseudocerasus_HiC_scaffold_1_3492 was opposite to the anthocyanin accumulation in fruits with different colors. It was expressed at low levels in the roots, stems, leaves, and flowers. Additionally, Ppseudocerasus_HiC_scaffold_6_1865/ 3_1684/ 8_2974 exhibited much lower expression in fruits compared to other tissues. Therefore, Ppseudocerasus_HiC_scaffold_3_1741 and 1_3492 are likely to play important roles in regulating anthocyanin biosynthesis in Chinese cherry fruits and are ideal candidate genes for further functional analysis. Based on phylogenetic analysis, the former gene exhibits a high degree of sequence similarity (65.20%~82.00%) with Rosaceae *MYB10s* (Fig. S5A). The latter one belongs to the FaMYB1-like type, exhibiting the highest sequence similarity (98.40%) with peach *PpMYB18* and sweet cherry *PavMYB4* (Fig. S5B). Therefore, they were renamed *CpMYB10* and *CpMYB4*, respectively.

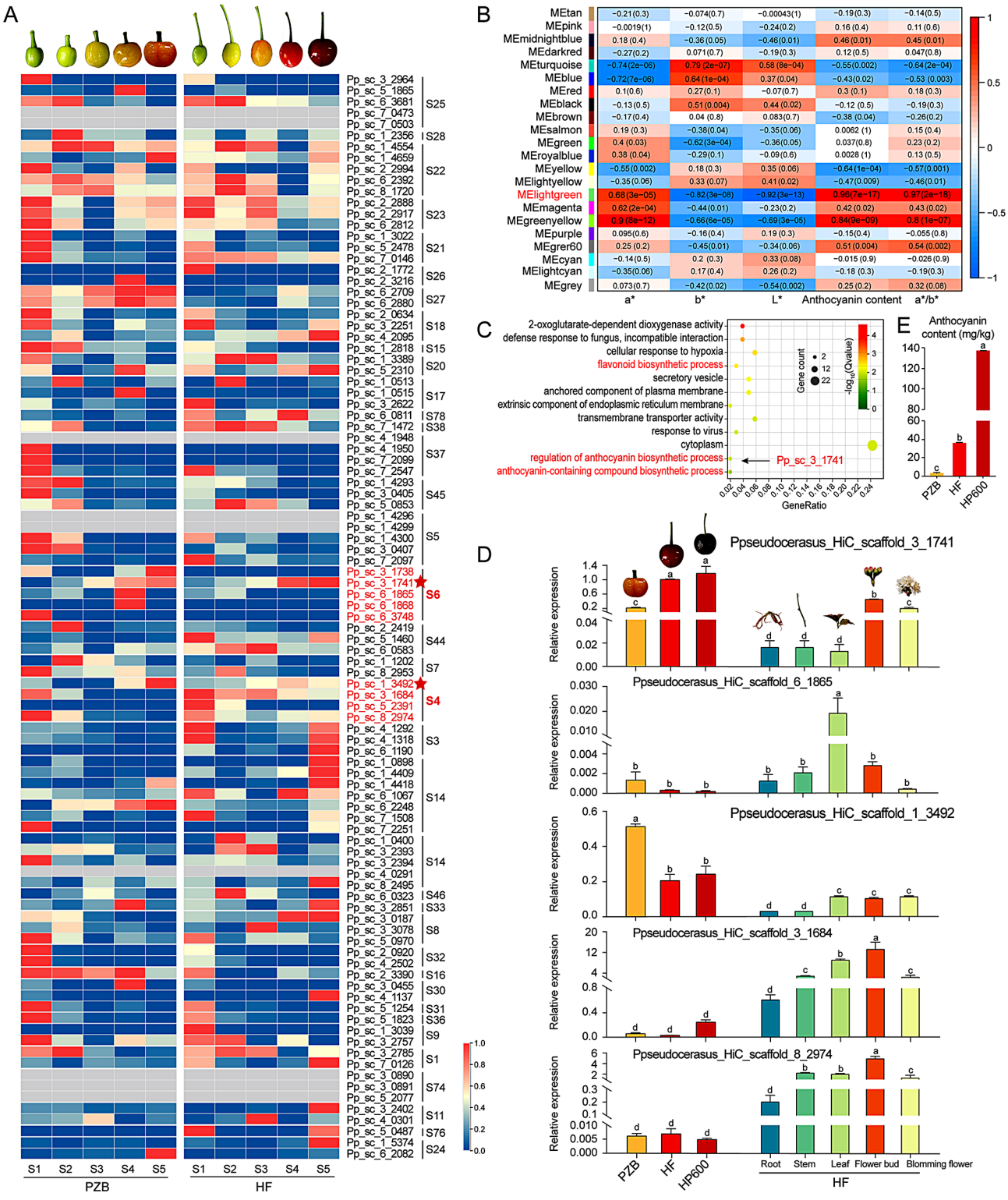

Fig. 3 Transcriptome profiling and relative expression of candidate *CpMYBs* associated with anthocyanin biosynthesis in Chinese cherry fruits. (**A**) Expression heatmap of *CpMYBs* during fruit development in yellow and red fruits. The color scale represents log_2-transformed FPKM values from 0 (blue) to 1 (red). (**B**) WGCNA based on the gene expression level and phenotypic data. The color scale on the right shows module-trait correlations from − 1 (blue) to 1 (red). (**C**) KEGG enrichment analysis of lightgreen module genes. (**D**) RT-qPCR validation of candidate genes related to anthocyanin biosynthesis in fruits with different colors and different tissues. (**E**) Anthocyanin content in matured fruits with different colors. The data represent the means ± SD from three independent replicates. Lowercase letters indicated the significant difference at 0.05 level

Function verification of *CpMYB10* and *CpMYB4* in Chinese cherry fruits

Subcellular localization and transcriptional activation activity

We cloned the coding sequences of CpMYB10 and CpMYB4 proteins to creat plasmid constructs encoding fusion proteins. The empty vector harboring GFP and mCherry was used as a positive control, which showed a diffused distribution of green and red fluorescence signals throughout the entire cells and nucleus, respectively. The GFP fluorescence signals of CpMYB10::GFP fusion proteins were predominantly localized in the nucleus, whereas the signals of CpMYB4::GFP fusion proteins were predominantly localized in the nucleus and cytoplasm (Fig. 4). The results demonstrated that CpMYB10 is a nuclear-localized protein, while CpMYB4 is a both cytoplasm- and nucleus-localized protein.

To investigate the transcriptional activity of CpMYB10 and CpMYB4, a transactivation assay was performed in the yeast strain Y2HGold. We found that the yeast cells carrying the positive control and pGBKT7-CpMYB10 survived on SD-Trp/Ade/His/+X-α-Gal media, while the negative control and pGBKT7-CpMYB4 did not survive (Fig. 5). These results indicated that CpMYB10 had transcriptional activation activity in yeast cells, while CpMYB4 was not transcriptionally active.

Transient expression of *CpMYB10* and *CpMYB4*

The OE-CpMYB10 yellow fruits accumulated a significantly higher anthocyanin content, with a 3.81-fold elevation in the skin compared to the control (Fig. 6A-1, A-2). Contrarily, the fruit flesh was not highly pigmented (Fig. S6), suggesting a differential regulation of anthocyanin biosynthesis between skin and flesh in Chinese cherry. Intriguingly, co-infiltration of *CpMYB10* and *CpMYB4* resulted in the disappearance of red pigmentation in yellow fruits (Fig. 6A-1, A-2). RT-qPCR analysis revealed a significant upregulation (6.7 ~ 8.0-fold) of key structural genes, particularly LBGs (*CpDFR*, *CpANS*, and *CpUFGT*), in OE-CpMYB10 fruits. Similarly, *CpGSTF12*, which regulates anthocyanin transport, also showed upregulated expression (Fig. 6A-3). However, there were no noticeable differences in the expression levels of co-infiltrated fruits with *CpMYB10* and *CpMYB4* compared to control (Fig. 6A-3). Conversely, silencing of *CpMYB4* in yellow fruits generated a slight blush in the skin (Fig. 6B-1) and a moderate accumulation of anthocyanin (Fig. 6B-2), but the content did not reach the

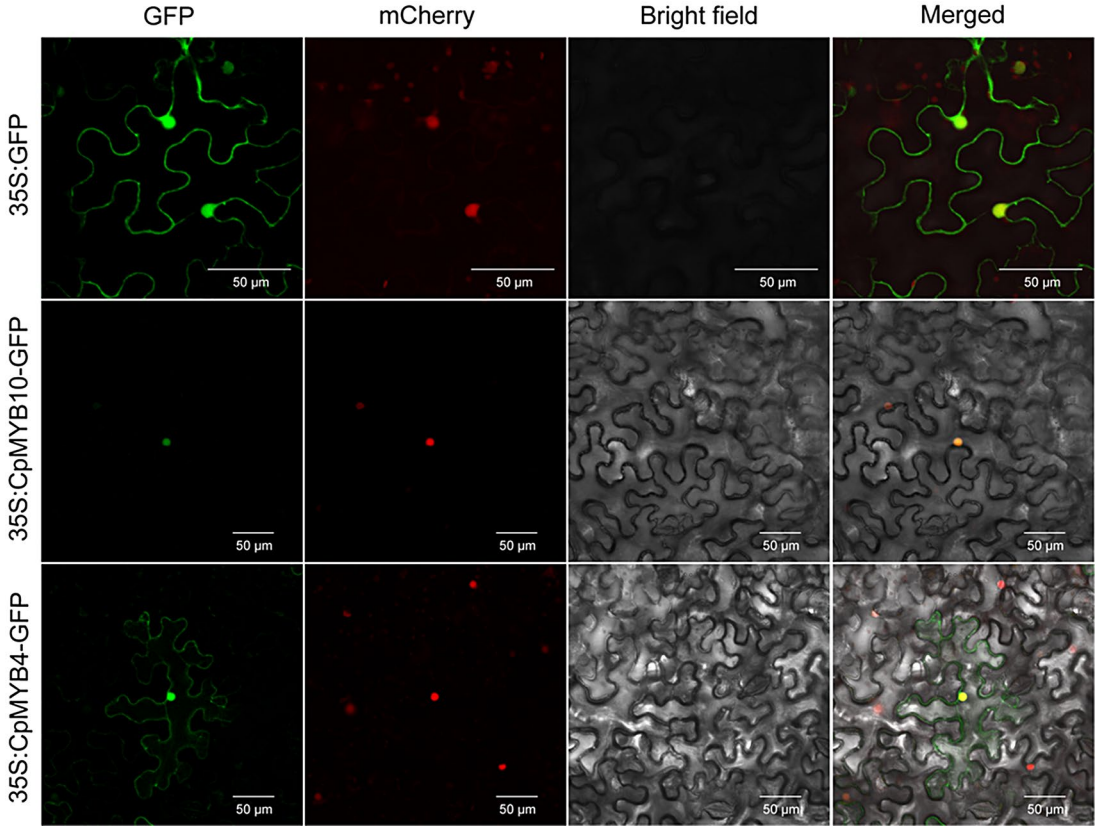

Fig. 4 Subcellular localization of the CpMYB10 and CpMYB4 proteins. The fusion constructs (35 S: CpMYB10-GFP, 35 S: CpMYB4-GFP) or an empty vector (35 S: GFP) were co-transformed with a nuclear marker gene, *VirD2NLS* fused to mCherry, in the epidermal cells of *Nicotiana benthamiana* leaves. GFP: green fluorescence; mCherry: red fluorescence; Bright Field: white light; Merged: combined GFP and mCherry signals. Bar = 50 μm

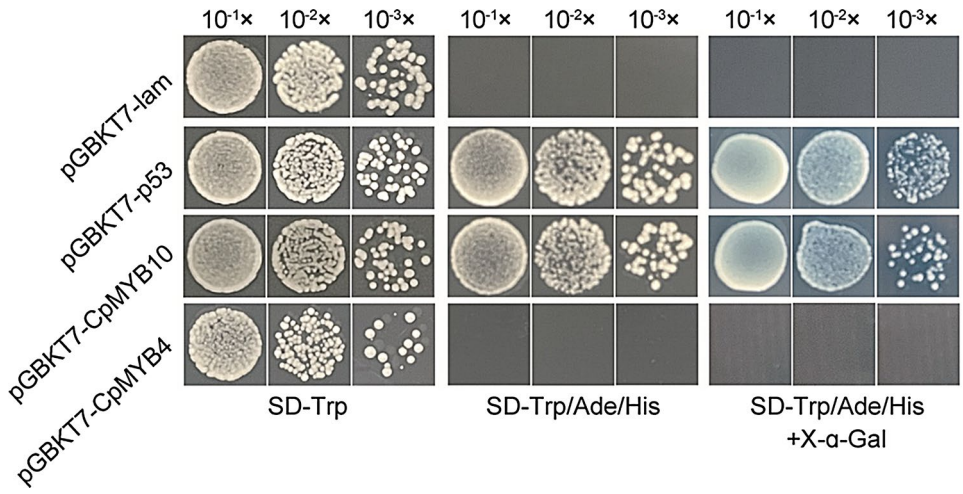

Fig. 5 Transactivation analysis of CpMYB10 and CpMYB4 using yeast assay. pGBKT7-CpMYB10/4: vector pGKBT7 containing CpMYB10/4. pGBKT7-p53, positive control; pGBKT7-lam, negative control

level observed in fully matured yellow fruits (Table S10). Expression analysis revealed a dramatical upregulation of both EBGs and LBGs, especially *CpUFGT* (51.7-fold) and *CpGSTF12* (21.3-fold), upon silencing *CpMYB4* (Fig. 6B-3). As expected, silencing of *CpMYB10* in red fruits led to a lighter skin color, significantly lower anthocyanin level (by 6.38-fold decrease), and downregulation of structural genes (Fig. 6C-1, C-Figs. 2 and C and 3). Collectively, these results support the hypothesis that *CpMYB10* acts as an activator, while *CpMYB4* functions as a repressor in the regulation of anthocyanin biosynthesis in Chinese cherry fruits.

Discussion

Species-specific expansion of *R2R3-MYB* gene family in Chinese cherry and its Rosaceae relatives

The MYB transcription factor family is the largest family in plants and plays a crucial role in regulating primary and secondary metabolism, growth and development, as well as hormone and stress responses [6]. Since its identification in *Arabidopsis* [47], whole-genome characterization of MYB TFs has been conducted in various plants, including strawberry [56], apple [57, 58], and sweet cherry [54]. In this study, we identified 1364 *R2R3-MYB* genes from Chinese cherry and 10 relatives in Rosaceae family, with the gene counts ranging from 99 to 134 in tribe Amygdaleae, and from 177 to 193 in tribe Maleae, 103 in tribe Potentilleae, and 98 in tribe Rubeae. The number of the *R2R3-MYB* gene family exhibited abundant diversity among these species, likely due to frequent gene duplications and losses. Notably, tribe Maleae species showed nearly twice as many genes as the other tribes, suggesting that a genome-wide duplication event in tribe Maleae might have led to the expansion of the *R2R3-MYB* gene family. This is also supported by the suggestion that *R2R3-MYB* genes have undergo rapid expansion during plant evolution via whole-genome duplication (WGD) and small-scale duplication [6]. Additionally, the gene numbers within identical subfamily also varied greatly among four cherry species, even though they are traditionally classified into *Cerasus* genus. This also implies species-specific expansion of *R2R3-MYB* gene family within the same genus.

In particular, the evolution of *R2R3-MYBs* in plants is related to specific expansions giving rise to species of lineage-specific subfamilies [59]. In this study, subfamily S45 exclusively contained *R2R3-MYB* genes from Chinese cherry and all relatives, indicating its unique role in Rosaceae family. Additionally, the absence of certain Rosaceae species in subfamilies S28, S15, S19, S13, S74, and S10 possibly suggests specific functions for these subfamilies. For instance, subfamilies S19, S13, and S10 were excluded only in Chinese cherry, indicating that they were lost during the evolution of Chinese cherry. S74 formed a subfamily with genes from all Rosaceae species except for strawberry, suggesting that these genes might play an important role only in woody plants. Furthermore, the subfamily S12 found in *Arabidopsis* was lost in Rosaceae, similar to observation in Solanaceae [60]. This further supports the notion that S12, involved in glucosinolates biosynthesis, is specific to the Brassicaceae family [61, 62]. Therefore, these results suggest an obvious expansion and functional trend toward specialized metabolism in *R2R3-MYB* gene family during the evolution of Chinese cherry and Rosaceae relative species.

CpMYB10 and *CpMYB4* are involved in anthocyanin biosynthesis in Chinese cherry

In this study, we identified 99 *CpMYB* genes of the R2R3 type within the genome of Chinese cherry. Based on the phylogenetic relationships and RNA-seq results, we selected five TFs from subfamilies S6 and S4 that may

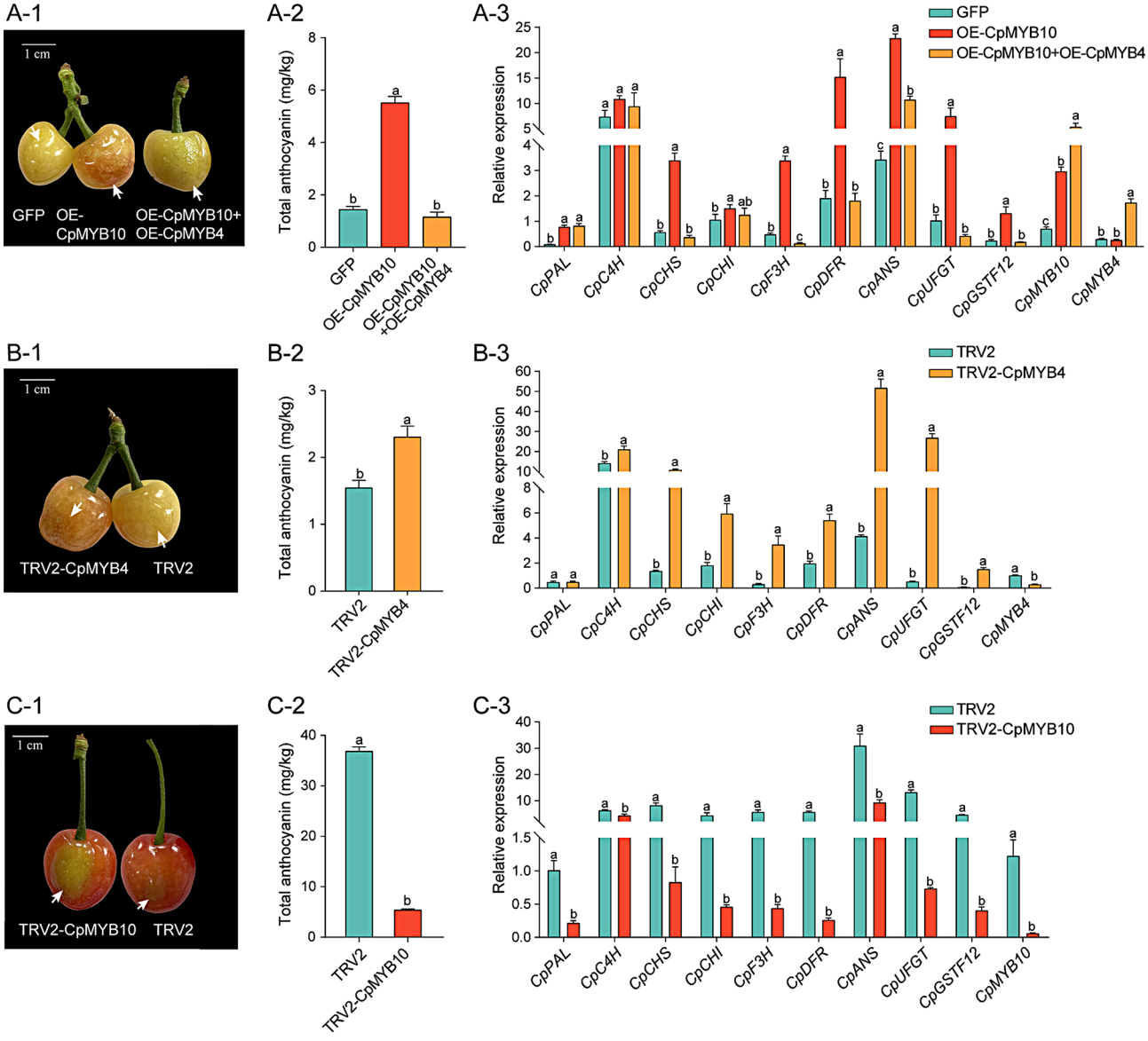

Fig. 6 Function verification of *CpMYB10* and *CpMYB4* in Chinese cherry fruits with different colors. (**A**), (**B**) and (**C**) Transient overexpression of *CpMYB10* and co-infiltration of *CpMYB10* and *CpMYB4* in yellow fruits, VIGS of *CpMYB4* in yellow fruits, and VIGS of *CpMYB10* in red fruits, respectively. (**1**) Fruit phenotypes after infiltration. The arrows indicate the infiltration sites. (**2**) Anthocyanin content of infiltration sites. (**3**) Expression levels of *CpMYB10* and *CpMYB4*, anthocyanin biosynthetic pathway genes and transporter gene in infiltration sites. The data represent the means ± SD obtained from RT-qPCR. Lowercase letters indicate the significant difference at 0.05 level

be involved in anthocyanin biosynthesis pathway. The expression level of *CpMYB10* increased rapidly during the fruit coloration stage and was higher in red fruits compared to yellow fruits. *CpMYB10* was also highly expressed in red flower buds. Conversely, the expression pattern of *CpMYB4* increased at the coloration stage in yellow fruits, while it decreased in red fruits. Both genes exhibited low expression levels in roots, stems, and leaves, indicating their specific expression is dependent on tissue type and ripeness stage, which is similar to the findings in sweet cherry [10, 54]. Transient overexpression of *CpMYB10* resulted in a 3.81-fold increase in anthocyanin level in yellow fruits (Fig. 6A-2), while silencing its expression led to a significant 6.38-fold decrease in anthocyanin content in red fruits (Fig. 6C-2). *CpMYB10* shares 81.50% of sequence similarity with sweet cherry *PavMYB10*, underscoring its pivotal role in regulating anthocyanin biosynthesis in Chinese cherry fruits. In contrast, silencing of *CpMYB4* only slightly rescued anthocyanin accumulation in yellow fruits (Fig. 6B-2), and its overexpression did not significantly alter anthocyanin content or color of red fruits (Fig. S7). This suggests that *CpMYB4* may not be the primary factor

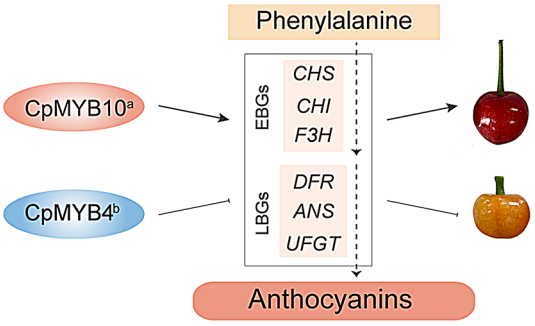

Fig. 7 Diagram of *CpMYB10* and *CpMYB4* involving in Chinese cherry fruit coloring. [a]*CpMYB10* may regulate anthocyanin biosynthesis in the skin by forming MBW complexes to activate the expression of structural genes. [b]*CpMYB4* may act as a corepressor, which is incorporated into or binds MBW complexes to change the complex activity and transform from activation to inhibition. *CHS*: chalcone synthase; *CHI*: chalcone isomerase; *F3H*: flavanone 3-hydroxylase; *DFR*: dihydroflavonol 4-reductase; *ANS*: leucoanthocyanidin dioxygenase; *UFGT*: flavonoid- 3-O-glucosyltransferase

contributing to the formation of yellow fruits in Chinese cherry.

Based on these results, we propose a model for the regulation of anthocyanin biosynthesis in Chinese cherry involving *CpMYB10* and *CpMYB4* (Fig. 7). *CpMYB10*, a member of the subfamily S6, may regulate anthocyanin biosynthesis in the skin by forming MBW complexes to activate the expression of structural genes, particularly the LBGs. Similarly, sweet cherry *PavMYB10.1a* interacts with *PavbHLH* and *PavWD40*, which is selectively recruited to the *PavANS* and *PavUFGT* promoter regions to enhance anthocyanin accumulation [10]. *FaMYB10* boosts anthocyanins accumulation by upregulating the expression of almost all structural genes in strawberry fruits [63]. Furthermore, the degree of trans-activation and interaction with bHLH partners varies greatly among *MYB10* genes in different Rosaceae species [17]. For instance, the efficient induction of anthocyanin biosynthesis by *MdMYB10* in apple depends on the co-expression of *MdbHLH3* and *MdbHLH33* [17, 64]. However, *MYB10* TFs perform poorly with *bHLH3* in some species such as peach, strawberry, and pear [17], and *FaMYB10* does not interact with *FabHLH33* in strawberry [63]. Additionally, variations in the promoter region of *MYB10* caused by the insertion of transposons or fragments alter gene expression, leading to activation or inactivation, thereby regulating coloration of Rosaceae fruits [11, 65, 66]. Thus, further study is needed to illustrate the regulation mechanism of *CpMYB10* activator responsible for anthocyanin accumulation in Chinese cherry.

CpMYB4 belongs to the FaMYB1-like type, which may act on the MBW complex to inhibit its activation [27]. Apple *MdMYB15L* weakens *MdbHLH33*-induced anthocyanin accumulation by interacting with *MdbHLH33* [31]. In peach, *PpMYB18*-like genes are likely to be induced by anthocyanin-related activators, thus providing negative feed regulation to MBW complexes and preventing the over-accumulation of anthocyanins [67]. As mentioned above, *CpMYB4* may be a minor factor that inhibits anthocyanin biosynthesis in Chinese cherry. The regulatory role and molecular mechanism of *CpMYB4* underlying anthocyanin accumulation also need further exploration. As previously reported, matured yellow fruit in Chinese cherry is not pure in color but exhibits a slight blush [4], suggesting the anthocyanin biosynthetic pathway is functional in yellow fruit. The formation of yellow fruit skin color might be a complex process that requires further in-depth study. Overall, this study provides a theoretical basis for further understanding the function of MYB family members in the process of Chinese cheery coloring.

Conclusions

This study presents a comprehensive and systematic analysis of the *R2R3-MYB* gene family in Chinese cherry and its Rosaceae relatives. A total of 1490 *R2R3-MYB* genes were identified and divided into 43 subfamilies across Chinese cherry, 10 Rosaceae relatives and *Arabidopsis*. The variation in gene numbers within identical subfamilies among different species, and the absence of certain subfamilies in some species, suggest species-specific expansion within the MYB gene family in Chinese cherry and its relatives. The expansion of *CpMYBs* was primarily driven by segmental and tandem duplication events. Phylogenetic relationships and transcript profiling further revealed *CpMYB10* and *CpMYB4* as key regulators involved in anthocyanin biosynthesis in Chinese cherry. Combined expressions patterns and function verification confirmed that *CpMYB10* promotes anthocyanin accumulation in the fruit skin, while *CpMYB4* acts as a minor repressor inhibiting anthocyanin biosynthesis in Chinese cherry. Further documentation is required to fully understand their authentic roles and regulatory mechanisms in Chinese cherry.

Supplementary Information

The online version contains supplementary material available at https://doi.org/10.1186/s12864-024-10675-7.

Supplementary Material 1

Supplementary Material 2

Acknowledgements

This work was supported by High-performance Computing Platform of Sichuan Agricultural University.

Author contributions

X.W. designed the experiments. Y.W. performed formal analysis and data curation. H.X.T. and J.Z. performed the experiments and data analysis. Y.W. and H.X.T. wrote the main manuscript text. H.W. performed plant materials management. Z.L. and J.T.Z. collected samples. W.H. Y.X.L. Y.T.Z. and M.L. conducted resources and validation. Z.W. performed project administration.

Q.C. Y.Z. Y.L. and H.R.T. supervised this work. X.W. revised the manuscript. All authors reviewed the manuscript.

Funding
This work was financially supported by Cherry Resources Sharing and Service Platform of Sichuan Province, Sichuan Science and Technology Program (2024YFHZ0302), Natural Science Foundation of Sichuan Province (2023NSFSC0158), Tianfu Talent Project of Chengdu City (2021-CF02-0162396-RC-4096), The Project of Rural Revitalization Research Institute in Tianfu New Area of Sichuan Province (XZY1-04), and Major Agricultural Technology Synergistic Promotion Program in 2023 (N[2023]—2132).

Data availability
The datasets supporting the results of this article are included with manuscript and available on request (Prof. Xiaorong Wang). Transcriptomic data during fruit development in yellow and red fruits of Chinese cherry is available in the CNGB database: CNP0003682.

Declarations

Ethics approval and consent to participate
All of the materials is owned by the authors and/or no permissions are required and they complied with the relevant institutional, national, and international guidelines and legislation. These methods were carried out in accordance with relevant guidelines and regulations.

Consent for publication
Not applicable.

Competing interests
The authors declare no competing interests.

Author details
[1]College of Horticulture, Sichuan Agricultural University, Chengdu, Sichuan 611130, China
[2]Key Laboratory of Agricultural Bioinformatics (Ministry of Education), Sichuan Agricultural University, Chengdu, Sichuan 611130, China

Received: 27 February 2024 / Accepted: 30 July 2024
Published online: 13 August 2024

References

1. Yü DJ, Lu LT, Ku TC, Li CL, Chen SX. Flora of China. Beijing: Science; 1986.
2. Huang XJ, Wang XR, Chen T, Chen J, Tang HR. Research progress of genetic diversity in *Cerasus pseudocerasus* and their wild relative populations, and utilize progress of cultivation resources. J Fruit Sci. 2013;30(3):470–9. https://doi.org/10.13925/j.cnki.gsxb.2013.03.024.
3. Wang Y, Du HM, Zhang J, Chen T, Chen Q, Tang HR, Wang XR. Ploidy level of Chinese cherry (*Cerasus Pseudocerasus* Lindl.) And comparative study on karyotypes with four *Cerasus* species. Sci Hortic. 2018;232:46–51. https://doi.org/10.1016/j.scienta.2017.12.065.
4. Wang Y, Hu GP, Liu ZS, Zhang J, Ma L, Tian T, Wang H, Chen T, Chen Q, He W, Yang SF, Lin YX, Zhang YT, Li MY, Zhang Y, Luo Y, Tang HR, Wang XR. Phenotyping in flower and main fruit traits of Chinese cherry [*Cerasus Pseudocerasus*. (Lindl) G Don] Sci Hortic. 2022;296:110920. https://doi.org/10.1016/j.scienta.2022.110920.
5. Allan AC, Hellens RP, Laing WA. MYB transcription factors that Colour our fruit. Trends Plant Sci. 2008;13(3):99–102. https://doi.org/10.1016/j.tplants.2007.11.012.
6. Wu Y, Wen J, Xia YP, Zhang LS, Du H. Evolution and functional diversification of R2R3-MYB transcription factors in plants. Hortic Res. 2022;9:uhac058. https://doi.org/10.1093/hr/uhac058.
7. Takos AM, Jaffe FW, Jacob SR, Bogs J, Robinson SP, Walker AR. Light-induced expression of a *MYB* gene regulates anthocyanin biosynthesis in red apples. Plant Physiol. 2006;142(3):1216–32. https://doi.org/10.1104/pp.106.088104.
8. Ban Y, Honda C, Hatsuyama Y, Igarashi M, Bessho H, Moriguchi T. Isolation and functional analysis of a MYB transcription factor gene that is a key regulator for the development of red colouration in apple skin. Plant Cell Physiol. 2007;48(7):958–70. https://doi.org/10.1093/pcp/pcm066.
9. Telias A, Lin-Wang K, Stevenson DE, Cooney JM, Hellens RP, Allan AC, Hoover EE, Braseen JM. Apple skin patterning is associated with differential expression of *MYB10*. BMC Plant Biol. 2011;11:93. https://doi.org/10.1186/1471-2229-11-93.
10. Jin WM, Wang H, Li MF, Wang J, Yang Y, Zhang XM, Yan GH, Zhang H, Liu JS, Zhang KC. The R2R3 MYB transcription factor *PavMYB10.1* involves in anthocyanin biosynthesis and determines fruit skin colour in sweet cherry (*Prunus avium* L). Plant Biotechnol J. 2016;14(11):2120–33. https://doi.org/10.1111/pbi.12568.
11. Castillejo C, Waurich V, Wagner H, Ramos R, Oiza N, Muñoz P, Triviño JC, Caruana J, Liu ZC, Cobo N, Hardigan MA, Knapp SJ, Vallarino JG, Osorio S, MartíN-Pizarro C, Posé D, Toivainen T, Hytönen T, Oh Y, Barbey CR, Whitaker VM, Lee S, Olbricht K, Sánchez-Sevilla JF, Amaya I. Allelic variation of *MYB10* is the major force controlling natural variation in skin and flesh color in strawberry (*Fragaria* spp.) fruit. Plant Cell. 2020;32(12):3723–49. https://doi.org/10.1105/tpc.20.00474.
12. Montefiori M, Brendolise C, Dare AP, Lin-Wang K, Davies KM, Hellens RP, Allan AC. In the Solanaceae, a hierarchy of bHLHs confer distinct target specificity to the anthocyanin regulatory complex. J Exp Bot. 2015;66(5):1427–36. https://doi.org/10.1093/jxb/eru494.
13. Naing AH, Kim CK. Roles of R2R3-MYB transcription factors in transcriptional regulation of anthocyanin biosynthesis in horticultural plants. Plant Mol Biol. 2018;98:1–18. https://doi.org/10.1007/s11103-018-0771-4.
14. Yan HL, Pei XN, Zhang H, Li X, Zhang XX, Zhao MH, Chiang VL, Sederoff RR, Zhao XY. MYB-mediated regulation of anthocyanin biosynthesis. Int J Mol Sci. 2021;22(6):3103. https://doi.org/10.3390/ijms22063103.
15. Dubos C, Stracke R, Grotewold E, Weisshaar B, Martin C, Lepiniec L. MYB transcription factors in Arabidopsis. Trends Plant Sci. 2010;15(10):573–81. https://doi.org/10.1016/j.tplants.2010.06.005.
16. Espley RV, Hellens RP, Putterill J, Stevenson DE, Kutty-Amma S, Allan AC. Red colouration in apple fruit is due to the activity of the MYB transcription factor, *MdMYB10*. Plant J. 2007;49(3):414–27. https://doi.org/10.1111/j.1365-313X.2006.02964.x.
17. Lin-Wang K, Bolitho K, Grafton K, Kortstee A, Karunairetnam S, Mcghie TK, Espley RV, Hellens RP, Allan AC. An R2R3 MYB transcription factor associated with regulation of the anthocyanin biosynthetic pathway in Rosaceae. BMC Plant Biol. 2010;10:50. http://www.biomedcentral.com/1471-2229/10/50
18. Lin-Wang K, Mcghie TK, Wang M, Liu Y, Warren B, Storey R, Espley RV, Allan AC. Engineering the anthocyanin regulatory complex of strawberry (*Fragaria vesca*). Front. Plant Sci. 2014;5:651. https://doi.org/10.3389/fpls.2014.00651.
19. Jiang LY, Yue ML, Liu YQ, Zhang NT, Lin YX, Zhang YT, Wang Y, Li MY, Luo Y, Zhang Y, Wang XR, Chen Q, Tang HR. A novel R2R3-MYB transcription factor FaMYB5 positively regulates anthocyanin and proanthocyanidin biosynthesis in cultivated strawberries (*Fragaria* × *ananassa*). Plant Biotechnol J. 2023;21(6):1140–58. https://doi.org/10.1111/pbi.14024.
20. Starkevic P, Paukstyte J, Kazanaviciute V, Denkovskiene E, Stanys V, Bendokas V, Siksnianas T, Razanskiene A, Razanskas R. Expression and anthocyanin biosynthesis-modulating potential of sweet cherry (*Prunus avium* L.) MYB10 and bHLH genes. PLoS ONE. 2015;10(5):e0126991. https://doi.org/10.1371/journal.pone.0126991.
21. Shen XJ, Zhao K, Liu LL, Zhang KC, Yuan HZ, Liao X, Wang Q, Guo XW, Li F, Li TH. A role for PacMYBA in ABA-regulated anthocyanin biosynthesis in red-colored sweet cherry cv. Hong Deng (*Prunus avium* L). Plant Cell Physiol. 2014;55(5):862–80. https://doi.org/10.1093/pcp/pcu013.
22. Lin-Wang K, Micheletti D, Palmer J, Volz R, Lozano L, Espley RV, Hellens RP, Chagné D, Rowan DD, Troggio M, Igarashi M, Allan AC. High temperature reduces apple fruit colour via modulation of the anthocyanin regulatory complex. Plant Cell Environ. 2011;34(7):1176–90. https://doi.org/10.1111/j.1365-3040.2011.02316.x.
23. Cavallini E, Tomas Matus J, Finezzo L, Zenoni S, Loyola R, Guzzo F, Schlechter R, Ageorges A, Arce-Johnson P, Tornielli GB. The phenylpropanoid pathway is controlled at different branches by a set of R2R3-MYB C2 repressors in grapevine. Plant Physiol. 2015;167(4):1448–552. https://doi.org/10.1104/pp.114.256172.
24. Xu HF, Wang N, Liu JX, Qu CZ, Wang YC, Jiang SH, Lu NL, Wang DY, Zhang ZY, Chen XS. The molecular mechanism underlying anthocyanin metabolism in apple using the *MdMYB16* and *MdbHLH33* genes. Plant Mol Biol. 2017;94:149–65. https://doi.org/10.1007/s11103-017-0601-0.
25. Jin HL, Cominelli E, Bailey P, Parr A, Mehrtens F, Jones J, Tonelli C. Transcriptional repression by AtMYB4 controls production of UV-protecting sunscreens in *Arabidopsis*. EMBO J. 2000;19(22):6150–61. https://doi.org/10.1093/emboj/19.22.6150.

26. Paolocci F, Robbins MP, Passeri V, Hauck B, Morris P, Rubini A, Arcioni S, Damiani F. The strawberry transcription factor *FaMYB1* inhibits the biosynthesis of proanthocyanidins in *Lotus corniculatus* leaves. J Exp Bot. 2011;62(3):1189–200. https://doi.org/10.1093/jxb/erq344.
27. Chen L, Hu B, Qin Y, Hu G, Zhao J. Advance of the negative regulation of anthocyanin biosynthesis by MYB transcription factors. Plant Physiol Biochem. 2019;136:178–87. https://doi.org/10.1016/j.plaphy.2019.01.024.
28. Xu HF, Zou Q, Yang GX, Jiang SH, Fang HC, Wang YC, Zhang J, Zhang ZY, Wang N, Chen XS. MdMYB6 regulates anthocyanin formation in apple both through direct inhibition of the biosynthesis pathway and through substrate removal. Hortic Res. 2020;7:72. https://doi.org/10.1038/s41438-020-0294-4.
29. Zhang L, Duan ZD, Ma S, Sun SK, Xiao YH, Ni N, Irfan M, Chen LJ, Sun YB. SlMYB7, an AtMYB4-Like R2R3-MYB transcription factor, inhibits anthocyanin accumulation in *Solanum lycopersicum* fruits. J Agric Food Chem. 2023;71(48):18758–68. https://doi.org/10.1021/acs.jafc.3c05185.
30. Jun JH, Liu C, Xiao X, Dixon RA. The transcriptional repressor MYB2 regulates both spatial and temporal patterns of proanthocyandin and anthocyanin pigmentation in *Medicago truncatula*. Plant Cell. 2015;27(10):2860–79. https://doi.org/10.1105/tpc.15.00476.
31. Xu HF, Yang GX, Zhang J, Wang YC, Zhang TL, Wang N, Jiang SH, Zhang ZY, Chen XS. Overexpression of a repressor MdMYB15L negatively regulates anthocyanin and cold tolerance in red-fleshed callus. Biochem Bioph Res Co. 2018;500(2):405–10. https://doi.org/10.1016/j.bbrc.2018.04.088.
32. Cao JP, Jiang Q, Lin JY, Li X, Sun CD, Chen KS. Physicochemical characterisation of four cherry species (*Prunus* spp.) grown in China. Food Chem. 2015;173:855–63. https://doi.org/10.1016/j.foodchem.2014.10.094.
33. Wang Y, Wang ZY, Zhang J, Liu ZS, Wang H, Tu HX, Zhou JT, Luo XR, Chen Q, He W, Yang SF, Li MY, Lin YX, Zhang YT, Zhang Y, Luo Y, Tang HR, Wang XR. Integrated transcriptome and metabolome analyses provide insights into the coloring mechanism of dark-red and yellow fruits in Chinese cherry [*Cerasus Pseudocerasus*. Int J Mol Sci. 2023;24(4):3471. https://doi.org/10.3390/ijms24043471.
34. Liu ZS, Wang H, Zhang J, Chen Q, He W, Zhang Y, Luo Y, Tang HR, Wang Y, Wang XR. Comparative metabolomics profiling highlights unique color variation and bitter taste formation of Chinese cherry fruits. Food Chem. 2024;439:138072. https://doi.org/10.1016/j.foodchem.2023.138072.
35. Arias R, Lee TC, Logendra L, Janes H. Correlation of lycopene measured by HPLC with the *L**, *a**, *b** color readings of a hydroponic tomato and the relationship of maturity with color and lycopene content. J. Agric. Food Chem. 2000;48(5):1697–702. https://doi.org/10.1021/jf990974e
36. Lee J, Durst RW, Wrolstad RE. Determination of total monomeric anthocyanin pigment content of fruit juices, beverages, natural colorants, and wines by the pH differential method: collaborative study. J Aoac Int. 2005;88(5):1269–78. https://doi.org/10.1093/jaoac/88.5.1269.
37. Wang JW, Liu WZ, Zhu DZ, Hong P, Zhang SZ, Xiao SJ, Tan Y, Chen X, Xu L, Zong XJ, Zhang LS, Wei HR, Yuan XH, Liu QZ. Chromosome-scale genome assembly of sweet cherry (*Prunus avium* L.) cv. Tieton obtained using long-read and Hi-C sequencing. Hortic Res. 2020;7:122. https://doi.org/10.1038/s41438-020-00343-8.
38. Baek S, Choi K, Kim GB, Yu HJ, Cho A, Jang H, Kim CK, Kim HJ, Chang KS, Kim JH, Mun JH. Draft genome sequence of wild *Prunus yedoensis* reveals massive inter-specific hybridization between sympatric flowering cherries. Genome Biol. 2018;19:127. https://doi.org/10.1186/s13059-018-1497-y.
39. Yi XG, Yu XQ, Chen J, Zhang M, Liu SW, Zhu H, Li M, Duan YF, Chen L, Wu L, Zhu S, Sun ZS, Liu XH, Wang XR. The genome of Chinese flowering cherry (*Cerasus serrulata*) provides new insights into *Cerasus* species Hortic. Res. 2020;7:165. https://doi.org/10.1038/s41438-020-00382-1
40. Fang ZZ, Wang KL, Dai H, Zhou DR, Jiang CC, Espley RV, Deng C, Lin YJ, Pan SL, Ye XF. The genome of low-chill Chinese plum Sanyueli (*Prunus salicina* Lindl.) Provides insights into the regulation of the chilling requirement of flower buds. Mol Ecol Resour. 2022;22(5):1919–38. https://doi.org/10.1111/1755-0998.13585.
41. Groppi A, Liu S, Cornille A, Decroocq S, Bui QT, Tricon D, Cruaud C, Arribat S, Belser C, Marande W, Salse J, Huneau C, Rodde N, Rhalloussi W, Cauet S, Istace B, Denis E, Carrère S, Audergon JM, Roch G, Lambert P, Zhebentyayeva T, Liu WS, Bouchez O, Lopez-Roques C, Serre RF, Debuchy R, Tran J, Wincker P, Chen XL, Pétriacq P, Barre A, Nikolski M, Aury JM, Abbott AG, Giraud T, Decroocq V. Population genomics of apricots unravels domestication history and adaptive events. Nat Commun. 2021;12:3956. https://doi.org/10.1038/s41467-021-24283-6.
42. Verde I, Jenkins J, Dondini L, Micali S, Pagliarani G, Vendramin E, Paris R, Aramini V, Gazza L, Rossini L, Bassi D, Troggio M, Shu S, Grimwood J, Tartarini S, Dettori MT, Schmutz J. The Peach v2.0 release: high-resolution linkage mapping and deep resequencing improve chromosome-scale assembly and contiguity. BMC Genomics. 2017;18:225. https://doi.org/10.1186/s12864-017-3606-9.
43. Shirasawa K, Itai A, Isobe S. Chromosome-scale genome assembly of Japanese pear (*Pyrus pyrifolia*) variety 'Nijisseiki'. DNA Res. 2021;28(2):dsab001. https://doi.org/10.1093/dnares/dsab001.
44. Sun XP, Jiao C, Schwaninger H, Chao CT, Ma Y, Duan NB, Khan A, Ban S, Xu K, Cheng LL, Zhong GY, Fei ZJ. Phased diploid genome assemblies and pan-genomes provide insights into the genetic history of apple domestication. Nat Genet. 2020;52:1423–32. https://doi.org/10.1038/s41588-020-00723-9.
45. Edger PP, Vanburen R, Colle M, Poorten TJ, Wai C, Niederhuth CE, Alger E, Ou S, Acharya CB, Wang J, Callow P, Mckain MR, Shi J, Collier C, Xiong Z, Mower JP, Slovin JP, Hytönen T, Jiang N, Childs KL, Knapp SJ. Single-molecule sequencing and optical mapping yields an improved genome of woodland strawberry (*Fragaria vesca*) with chromosome-scale contiguity. GigaScience. 2017;7(2):gix124. https://doi.org/10.1093/gigascience/gix124.
46. Vanburen R, Wai CM, Colle M, Wang J, Sullivan S, Bushakra JM, Liachko I, Vining KJ, Dossett M, Finn CE, Jibran R, Chagné D, Childs K, Edger PP, Mockler TC, Bassil NV. A near complete, chromosome-scale assembly of the black raspberry (*Rubus occidentalis*) genome. GigaScience. 2018;7(8):giy094. https://doi.org/10.1093/gigascience/giy094.
47. Stracke R, Werber M, Weisshaar B. The R2R3-MYB gene family in Arabidopsis thaliana. Curr Opin Plant Biol. 2001;4(5):447–56. https://doi.org/10.1016/S1369-5266(00)00199-0.
48. Chen CJ, Chen H, Zhang Y, Thomas HR, Frank MH, He YH, Xia R. TBtools: an integrative toolkit developed for interactive analyses of big biological data. Mol Plant. 2020;13:1194–202. https://doi.org/10.1016/j.molp.2020.06.009.
49. Wang Y, Tang H, Debarry JD, Tan X, Li J, Wang X, Lee T, Jin H, Marler B, Guo H, Kissinger JC, Paterson AH. MCScanX: a toolkit for detection and evolutionary analysis of gene synteny and collinearity. Nucleic Acids Res. 2012;40(7):e49. https://doi.org/10.1093/nar/gkr1293.
50. Lin YX, Jiang LY, Chen Q, Li YL, Zhang YT, Luo Y, Zhang Y, Sun B, Wang XR, Tang HR. Comparative transcriptome profiling analysis of red-and white-fleshed strawberry (*Fragaria* × *ananassa*) provides new insight into the regulation of the anthocyanin pathway. Plant Cell Physiol. 2018;59(9):1844–59. https://doi.org/10.1093/pcp/pcy098.
51. Dong YX, Qi XL, Liu CL, Song LL, Li M. A sweet cherry AGAMOUS-LIKE transcription factor *PavAGL15* affects fruit size by directly repressing the *PavCYP78A9* expression. Sci Hortic. 2022;297:110947. https://doi.org/10.1016/j.scienta.2022.110947.
52. Li PF, Wen J, Chen P, Guo PC, Ke YZ, Wang MM, Liu MM, Tran LSP, Li JN, Du H. MYB superfamily in *Brassica napus*: evidence for hormone-mediated expression profiles, large expansion, and functions in root hair development. Biomolecules. 2020;10:875. https://doi.org/10.3390/biom10060875.
53. Xu WJ, Dubos C, Lepiniec L. Transcriptional control of flavonoid biosynthesis by MYB-bHLH-WDR complexes. Trends Plant Sci. 2015;20(3):176–85. https://doi.org/10.1016/j.tplants.2014.12.001.
54. Sabir IA, Manzoor MA, Shah IH, Liu XJ, Zahid MS, Jiu ST, Wang JY, Abdullah M, Zhang CX. MYB transcription factor family in sweet cherry (*Prunus avium* L.): genome-wide investigation, evolution, structure, characterization and expression patterns. BMC Plant Biol. 2022;22:2. https://doi.org/10.1186/s12870-021-03374-y.
55. Fawcett JA, Maere S, Van De Peer Y. Plants with double genomes might have had a better chance to survive the cretaceous–tertiary extinction. P Natl Acad Sci USA. 2009;106(14):5737–42. https://doi.org/10.1073/pnas.0900906106.
56. Liu H, Xiong JS, Jiang YT, Wang L, Cheng ZM. Evolution of the R2R3-MYB gene family in six Rosaceae species and expression in woodland strawberry. J Integr Agr. 2019;18(12):2753–70. https://doi.org/10.1016/S2095-3119(19)62818-2.
57. Cao ZH, Zhang SZ, Wang RK, Zhang RF, Hao YJ. Genome wide analysis of the apple MYB transcription factor family allows the identification of MdoMYB121 gene confering abiotic stress tolerance in plants. PLoS ONE. 2013;8(7):e69955. https://doi.org/10.1371/journal.pone.0069955.
58. Ding Y, Yang QH, Waheed A, Zhao MQ, Liu XJ, Kahar G, Haxim Y, Wen XJ, Zhang DY. Genome-wide characterization and functional identification of MYB genes in *Malus sieversii* infected by *Valsa Mali*. Front Plant Sci. 2023;14:1112681. https://doi.org/10.3389/fpls.2023.1112681.
59. Soler M, Oliveira Camargo EL, Carocha V, Cassan-Wang H, Clemente HS, Savelli B, Hefer CA, Pinto Paiva JA, Myburg AA, Grima-Pettenati J. The *Eucalyptus grandis* R2R3-MYB transcription factor family: evidence for woody

growth-related evolution and function. New Phytol. 2015;206(4):1364–77. https://doi.org/10.1111/nph.13039.
60. Yin Y, Guo C, Shi HY, Zhao JH, Ma F, An W, He XR, Luo Q, Cao YL, Zhan XQ. Genome-wide comparative analysis of the *R2R3-MYB* gene family in five Solanaceae species and identification of members regulating carotenoid biosynthesis in wolfberry. Int J Mol Sci. 2022;23(4):2259. https://doi.org/10.3390/ijms23042259.
61. Matus JT, Aquea F, Arce-Johnson P. Analysis of the grape *MYB R2R3* subfamily reveals expanded wine quality-related clades and conserved gene structure organization across *Vitis* and *Arabidopsis* genomes. BMC Plant Biol. 2008;8:83. https://doi.org/10.1186/1471-2229-8-83.
62. Seo MS, Jin M, Chun JH, Kim SJ, Park BS, Shon SH, Kim JS. Functional analysis of three *BrMYB28* transcription factors controlling the biosynthesis of glucosinolates in *Brassica rapa*. Plant Mol Biol. 2016;90:503–16. https://doi.org/10.1007/s11103-016-0437-z.
63. Yue ML, Jiang LY, Zhang NT, Zhang LX, Liu YQ, Lin YX, Zhang YT, Luo Y, Zhang Y, Wang Y, Li MY, Wang XR, Chen Q, Tang HR. Regulation of flavonoids in strawberry fruits by FaMYB5/FaMYB10 dominated MYB-bHLH-WD40 ternary complexes. Front Plant Sci. 2023;14:1145670. https://doi.org/10.3389/fpls.2023.1145670.
64. Xie XB, Li S, Zhang RF, Zhao J, Chen YC, Zhao Q, Yao YX, You CX, Zhang XS, Hao YJ. The bHLH transcription factor MdbHLH3 promotes anthocyanin accumulation and fruit colouration in response to low temperature in apples. Plant Cell Environ. 2012;35(11):1884–97. https://doi.org/10.1111/j.1365-3040.2012.02523.x.
65. Espley EV, Brendolise C, Chagné D, Kutty-Amma S, Green S, Volz R, Putterill J, Schouten HJ, Gardiner SE, Hellens RP, Allan AC. Multiple repeats of a promoter segment causes transcription factor autoregulation in red apples. Plant Cell. 2009;21(1):168–83. https://doi.org/10.1105/tpc.108.059329.
66. Guo J, Cao K, Deng C, Li Y, Zhu GR, Fang WC, Chen CW, Guan L, Wu S, Guo WW, Yao JL, Fei ZJ, Wang LR. An integrated peach genome structural variation map uncovers genes associated with fruit traits. Genome Biol. 2020;21:258. https://doi.org/10.1186/s13059-020-02169-y.
67. Zhou H, Lin-Wang K, Wang FR, Espley RV, Ren F, Zhao JB, Ogutu C, He HP, Jiang Q, Allan AC, Han YP. Activator-type R2R3-MYB genes induce a repressor-type R2R3-MYB gene to balance anthocyanin and proanthocyanidin accumulation. New Phytol. 2019;221(4):1919–34. https://doi.org/10.1111/nph.15486.

Publisher's Note